ZHOU ZHANG
SHENGWEI WANG
MIN ZHOU
and
BAOAN XIAN

Characteristics of a coal reservoir pore-fracture system and favourable reservoir selection in the Kuba coalfield, Xinjiang province, China

The Kuba coalfield in Xinjiang province is a new block for the exploration and development of coalbed methane in China, and in order to explore the coalbed methane recovery potential the coal reservoir pore-fracture system characteristics need to be researched, and favourable reservoir selection needs to be carried out. The pores, micro-fissures, and macro-fissures are studied as an organic whole. To characterize the physical properties and microscopic pores of coal reservoirs 4 sets of experiments are performed. A scanning electron microscope is used to study the development characteristics of micro-fissure systems; surface tectonic fissure mapping techniques and fine comparison of coal reservoirs in mines are conducted to study the endogenous and exogenous fissures. The characteristics of porosity and fissure are also studied, including the A coal seam group in the Tariqik formation, the Yangxia formation B coal seam and the Kizinur formation C coal seam. The results obtained in this study demonstrated that two coal seams in the Kuba coalfield, namely A5 and A7, are more favourable reservoirs compared to the other seams based on the perspective of pore-fissures, and these results provide a theoretical basis for coalbed methane exploration and development.

Keywords*: Coalbed methane; coal reservoir; pore-fracture system; reservoir selection; Kuba coalfield*

1. Introduction

The pore-fracture system of a coal reservoir is an important space for coalbed methane adsorption, diffusion and migration (Gamson et al., 1998; Shi and Durucan, 2005; Xu et al., 2005; Yao et al., 2009). Estimation of the pore-fracture system of coal-bearing strata has been applied widely in coalbed methane (CBM) exploration in many coal basins of the USA, Canada, Australia and China. A coal reservoir has a "double pore" structure composed of pores and fissures (Ayers, 2002), in which the matrix pore is the coalbed methane storage space, the macroscopic fissure is the coalbed methane migration channel, and the microscopic fissure is the bridge between the pore and the macroscopic fissure (Sang et al., 2005). The development feature of the pore and fracture system in a coal reservoir determines the permeability of the coal reservoir, affects the productivity of the coalbed methane development wells, and is the key factor in coalbed methane exploration and development (Li et al., 2013, 2014a). Natural fractures in coal are the most important physical attribute that governs gas flow in a CBM reservoir (Moore, 2012). Cleat spacing varies with coal rank, decreasing from lignite through medium volatile bituminuous coal (Law, 1993). A large number of structural fractures will be produced by the tectonic stress of coal rock, which will affect the permeability of the coal reservoir (Xue et al., 2012). In studying the physical characteristics of the coal reservoir in the Kuba coalfield, the pores, microfractures and macrofractures should be analyzed as a whole.

The total amount of coal resources in the Kuba coalfield is 19.7 billion tonnes, composed mainly of medium metamorphic coking coal, locally developed fat coking coal and lean coal, and the CBM resource quantity of 2000 m is estimated to be 227 billion m^3, and has good potential for coalbed methane exploration and development (Zhang, 2016). CBM resources in medium-rank coal are abundant in China, especially in the Ordos Basin (Tang et al., 2004; Li and Zhang, 2013; Meng et al., 2014). However, to date, few studies have investigated the physical properties of coal reservoirs in the Kuba coalfield in Xinjiang province, China. The vitrinite reflectance ranges from 0.7% to 1.82% in the Kuba coalfield. The pore-fracture characteristics of this area are quite different from those of the high-coal rank area, which has been successfully developed in the southern Qinshui basin in China (Cai et al., 2011; Tao et al., 2012; Lv et al., 2012).

In this study, experimental methods are used to study the porosity and microfissures, and surface structure fissure

Messrs. Zhou Zhang, Min Zhou, Baoan Xian, School of Resources and Environment, Henan Polytechnic University, Jiaozuo, Collaborative Innovation Center of Coalbed Methane and Shale Gas for Central Plains Economic Region, Henan Province, Jiaozuo, Henan International Joint Laboratory for Unconventional Energy Geology and Development, Jiaozuo, and Shengwei Wang, Faculty of Earth Resources, China University of Geosciences (Wuhan), Wuhan, China. E-mail: zhangzhou@hpu.edu.cn•iZ. Zhang•j, 348059103@hpu.edu.cn•iS.W. Wang•j, zhoumin@hpu.edu.cn•iM. Zhou j, 759267793@qq.com iB.A. Xian j

mapping technology and the mine method of coal reservoirs are applied to contrast the anatomical technology to study the cleats and exogenetic fissures in coal reservoirs. The main coal reservoirs that developed in the coalfield are selected and evaluated from the perspective of pores and fissures to aid in the exploration and development of coalbed methane in this area. Section 2 demonstrates the geological and tectonic background associated with the Kuba coalfield in China. In Section 3, all coal samples collected from the working faces of coal mines in the Kuba coalfield are presented, and the distribution of internal and external fractures in coal reservoirs are studied on the basis of mapping of the outcrop structural fractures. Furthermore, the experimental procedure pursued in this study is presented in this section. Section 4 discusses the results obtained, and Section 5 lists the main conclusions of this study.

2. Geological and tectonic background

The Kuba coalfield starts from Laohutai township in the west of Baicheng County and east of Kuqa River in Kuqa County, covering an area of approximately 1585 km^2. The administrative division belongs to Baicheng County and Kuqa County in the Aksu region, Xinjiang province. The Kuba coalfield is a monoclinic structure that has always been inclined to the south, and the stratigraphic strike is near east-west. The main structures of the coalfield are as follows: F_1 reverse fault in the north, F_2 and F_3 normal faults in the south, and Wuddick anticline and Wudike syncline in the south of the coalfield, which belong to the large fold type (Fig.1).

The Taliqike formation (J_1t) in the Kuba coalfield is the main coal-bearing formation. The average thickness of the rock strata is 148.58–281.84 m, the cumulative average thickness of the coal seam is 28.99 m, and the coal-bearing coefficient is 11.63%. Most mineable and sporadic mineable coal seams constitute 9 layers (A_1–A_9), and there are 6 layers of non-mineable coal seams (A_{10}–A_{15}). The Yangxia formation (J_1y) is also a coal-bearing formation, named the B coal formation. The single layer thickness of the coal seam is 0.05–5.61 m, and the average total thickness is 4.03 m. The coal seam

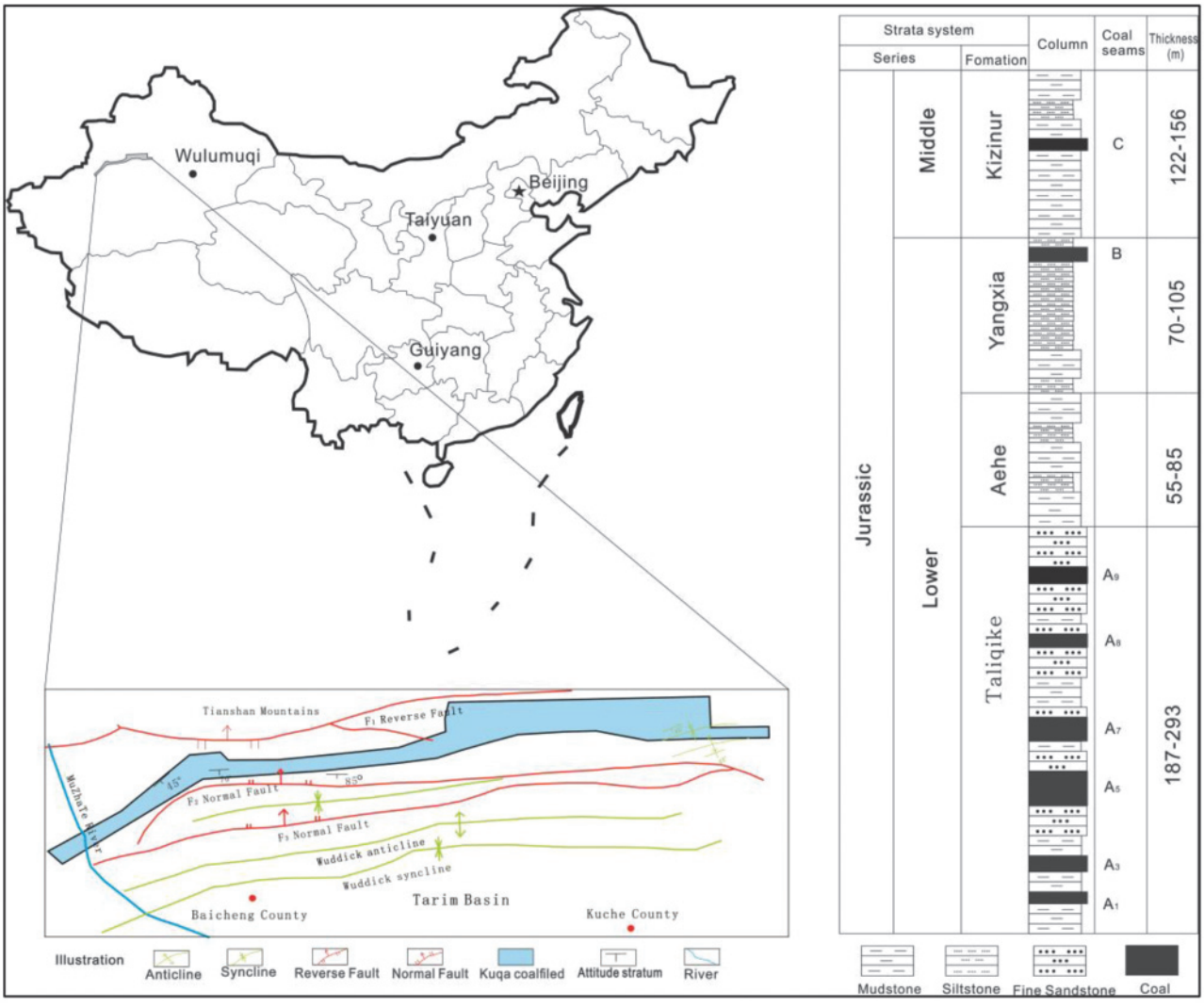

Fig.1 The distribution of tectonic units and stratum in the study area

Table 1 Basic testing data of coal in the Kuba coalfield

Target coal seams	Sample no.	True density (g/cm^3)	Ro(%)	Proximate analysis (%)				Coal maceral composition (%)			
				M, ad	A, d	V, daf	FC, ad	V	I	E	M
A_1	YZ001	1.72	0.73	0.53	22.00	9.36	68.11	71.20	21.00	-	7.80
	YZ002	1.60	0.76	0.86	28.00	10.28	60.86	70.50	21.30	-	8.20
	SF003	1.52	0.71	1.23	25.00	11.85	61.92	76.30	15.60	-	8.10
A_3	YZ004	1.48	0.78	0.65	4.21	13.30	81.84	78.58	17.92	-	3.50
	YZ005	1.45	0.74	0.68	4.45	13.98	80.89	80.69	13.71	-	5.60
	YZ006	1.56	0.76	0.70	4.88	14.58	79.84	81.47	11.33	-	7.20
	SF007	1.40	0.73	0.65	5.23	14.20	79.92	79.14	14.46	-	6.40
A_5	DWQ008	1.42	0.81	1.03	11.22	28.95	58.80	66.45	26.34	-	7.21
	DWQ009	1.45	0.80	1.16	14.71	25.12	58.01	69.85	23.15	1.80	5.20
	WZ010	1.46	0.78	1.14	13.87	27.32	55.67	64.31	24.99	2.50	8.20
	WZ011	1.40	0.77	1.18	12.30	29.30	53.22	60.47	30.43	-	9.10
	CT012	1.48	0.82	1.36	13.88	26.55	58.21	70.81	16.39	3.20	9.60
A_7	DWQ013	1.47	0.79	1.60	4.62	29.62	64.16	77.10	18.03	-	4.87
	DWQ014	1.45	0.80	1.20	10.24	30.23	58.33	79.25	16.33	1.20	3.22
	WZ015	1.48	0.81	1.45	11.69	31.58	55.28	81.11	11.74	-	7.15
	WZ016	1.42	0.80	1.50	15.36	34.55	38.59	80.75	13.60	-	5.65
	CT017	1.44	0.82	1.32	9.82	27.11	61.75	78.43	12.79	1.90	6.88
A_8	DWQ018	1.48	0.78	0.81	18.56	30.56	50.07	75.85	18.95	-	5.20
	DWQ019	1.45	0.80	0.85	21.11	31.14	46.9	74.13	19.42	0.95	5.50
	WZ020	1.40	0.72	0.80	20.28	28.85	50.07	78.90	16.28	-	4.82
	CT021	1.42	0.75	0.88	21.35	29.75	51.92	80.25	9.63	1.22	8.90
A_9	DWQ022	1.42	0.70	0.82	14.53	30.89	53.76	75.86	18.33	-	5.81
	DWQ023	1.48	0.72	0.76	10.25	33.50	55.49	72.30	20.87	-	6.83
	WZ024	1.46	0.75	0.69	8.56	36.27	54.48	72.71	17.38	0.91	9.00
B	YZ025	1.37	1.77	1.20	5.35	18.58	74.87	85.64	12.24	-	2.12
	YZ026	1.38	1.82	1.06	2.66	14.06	82.22	88.70	8.77	-	2.53
	YZ027	1.36	1.65	1.08	3.78	16.52	78.62	86.37	11.83	-	1.80
C	SF028	1.39	1.56	1.05	7.96	12.20	78.79	83.76	13.26	-	2.98
	SF029	1.40	1.45	0.94	6.05	19.29	73.72	85.52	11.07	-	3.41
	SF030	1.38	1.65	0.88	5.88	15.32	77.92	80.30	15.71	-	3.99

V: vitrinite; I: inertinite; E: exinite; M: minerals; M, ad: moisture (air-dried basis); A, d: ash (dry basis); V, daf: volatile (dry, ash free basis); FC, ad: fixed carbon (air-dried basis); Ro: vitrinite reflectance.

number and thickness vary greatly and can only be mined in the western part of the Kuba coalfield. The thickness of the middle Jurassic Kizinur formation (J_2k) is 265.00–860.00 m, and the average thickness is 487.00 m. The lower part contains coal and is named the C coal group. C_2 is a locally mineable coal seam (Table 1).

3. Samples and methods

3.1. Sample collection

In total, 27 coal samples were collected from the working faces of coal mines in the Kuba coalfield, and 3 coal samples are collected from coalbed methane well core samples. These samples basically cover the main target layer of coalbed methane exploration and development, including 6 from the Wenzhou coal mine, 8 from the Dawanqi coal mine, 5 from the Shunfa coal mine, 8 from the Yize coal mine and 3 from the coalbed methane well.

3.2. Field outcrop study

Based on the mapping of outcrop structural fractures in the field and the fine contrast technique of coal reservoirs under coal mines, the distribution of internal and external fractures in coal reservoirs can be studied. The outcrops of surrounding rocks and coal reservoirs in the study area are good. The exogenetic fractures can be observed directly, and coal mines are being exploited in the area, which provides a convenient condition for the study of macroscopic fractures.

The coalbed methane development block with an intact outcrop of coal measure is selected, and the folds, faults and structural fissures in the outcrop of the same tectonic layer are measured using surface high-precision structural fissure-mapping technology, which involves the following procedure:

Fig.2 Outcrop photos of coal seams and surrounding rocks in the study area

identify the detailed structural fissure mapping steps, clarify the identification marks of structural fissures in the field, and determine the parameters of the structural fissure mapping measurements, including point number, coordinates, attitude of the stratum, lithology, attitude of the rock, structural fissure occurrence, cutting relationship, opening, movement, mode of movement, filling characteristics, scale, and surface density (Fig.2).

Based on surface high-precision structural fissure mapping, the spacing of the observation points is 100–150 m, and the density of the observation points is approximately 100 per square kilometer. The reference standard is "Coalfield Geological Mapping Regulations" (DZ/T 0175-1997), for direct observation of the endogenous and exogenous fractures in outcrops of coal reservoirs. In addition, there are coal mines under exploitation in the study area, which is convenient for the observation of underground coal reservoir fractures. The spacing of the observation points is 1.10 m from the roadway, and the working face is excavated manually. A fine anatomical comparison technique is used to study the internal and external fissures in the underground coal reservoir.

3.3. Experimental work

To characterize the physical properties and microscopic pores of coal reservoirs in the Kuba coalfield, 4 sets of experiments are performed.

Set-I experiments are the proximate analysis tests. Proximate analysis is performed on all samples to measure the moisture content, the ash content and the volatile material content of the coal. A TJGF-3000 automatic industrial analyzer is used for the proximate analysis of the coal. The sample mass is 0.5–1g, and the temperature control accuracy is +5ºC. The test method is operated according to the national standard GB/T 212-2008.

In order to determine the degree of coal metamorphism, Set-II experiments are carried out. Set-II experiments included vitrinite reflectance (Ro) measurements and a coal maceral composition test. Ro measurements and coal maceral analyses are carried out on the same polished specimen using an LV100 POL photometer microscope with an E200 photosystem manufactured by the Leitz Company of Germany (following China National Standards GB/T 6948-2008 and GB/T 8899-1998, respectively).

To investigate the difference among the adsorption pore structure and CBM storage capacities of coal seams, Set-III experiments (including low-temperature N_2 isotherm adsorption/desorption analysis and mercury injection) are performed. The low-temperature N_2 isotherm adsorption/desorption analysis is carried out with a micromeritics ASAP-2000 automated surface area analyzer in accordance with the national standard GB/T 19587-2004. To carry out the low-temperature N_2 isotherm adsorption/desorption experiment, all coal samples are crushed and sieved to a size ranging between 0.23 and 0.45 mm and are then dried at 105ºC for 24 h in a vacuum oven. Each sample is measured under a relative pressure from 0.01 to 1 to obtain the BET pore surface area (S_{BET}), the BJH total pore volume (V_{BJH}), and the pore size distribution. The contents of pores in the coal samples are analyzed by mercury injection experiment. The mercury injection test is carried out with an Auto Pore IV 9500 VI.07 porosimeter. The maximum mercury injection pressure is 210 MPa, and the pore size and pore size distribution are quantitatively measured at a pore diameter greater than 7 nm, in addition to pore size distribution, porosity and other parameters. The mercury injection experiment is carried out in accordance with the national standard GB/T 21650-2008.

In an attempt to describe the shape, length, aperture and connectivity of micro-fractures under an optical microscope and scanning electron microscope (SEM), set-IV experiments are performed. The coal samples are divided into two groups of coal slices, and the processes are conducted as follows. The first group is incised and polished to a 30 mm × 30 mm cube, of which the surface is divided into 9 equal small zones of 10 mm × 10 mm that are used to determine the fracture amount and type in sequence using an LV100 POL microscope with a MPS 60 photometer system. In the second group, one side of the polished coal sample surface is gold-plated to increase the electrical conductivity, and these samples are examined under an FEI QUANTA 250 SEM. The microscope is equipped with a high performance X-ray energy spectrometer that simultaneously carried out

qualitative and semi-quantitative analysis of the elements of the surface layer of each sample to provide a comprehensive analysis of morphology and the chemical composition.

4. Results and discussion

4.1. Basic parameters of coal

The main exploration and exploitation CBM target coal seams in the Kuba coalfield are A_1, A_3, A_5, A_7, A_8 and A_9 in the Taliqike formation, B coal seams in the Yangxia formation and C coal seams in the Kizinur formation. Of the 8 coal samples collected from the Yize mine, 2 are from the A_1 coal seam, 3 are from the A_3 coal seam and 3 are from the B coal seam. In total, 5 coal samples are collected from the Shunfa mine; 1 of them is from the A1 coal seam, 1 is from the A_3 coal seam and 3 are from the C coal seam. Of the 8 coal samples collected from the Dawanqi mine, 2 are from the A_5 coal seam, 2 are from the A_7 coal seam, 2 are from the A_8 coal seam and 2 are from the A_9 coal seam. In total, 6 coal samples are collected from the Wenzhou Mine; 2 are from the A_5 coal seam, 2 are from the A_7 coal seam, 1 is from the A_8 coal seam and 1 is from the A_9 coal seam. The 3 core samples from the coalbed methane represented the A_5, A_7 and A_8 coal seams.

The coal samples in the Kuba coalfield ranged from gas coal to lean coal, and their Ro values ranged from 0.70–1.82% (Table 1). The Ro values of the A_1, A_3, A_5, A_7, A_8 and A_9 coal seams in the Taliqike formation ranged from 0.70–0.82%. These coal seams are mainly gas coal of medium metamorphism. The Ro value of the B coal seam in the Yangxia formation is 1.75%, and it is lean coal. The C coal seam is coking coal. The coal maceral composition test results showed that the vitrinite, inertinite and mineral contents had no relationship with the increase in coal rank. In addition, the exinite content is very low, most of the coal is not detected, and the small-coal content is approximately 1%. The ash content of coal seam A_1 is the highest, with an average of 25%, indicating medium to high ash coal. The high ash content in coal seam A_1 is unfavourable for the development of coalbed methane. The A_8 coal seam is similar; its ash content is 20%. A high ash content in a coal reservoir leads to a lower gas content of coalbed methane, which is unfavourable for coalbed methane development. Therefore, the A_1 and A_8 coal reservoirs are not favourable for coalbed methane development. The ash content of the other coal seams is less than 15%, which is appropriate for the development of coalbed methane (Fig.3).

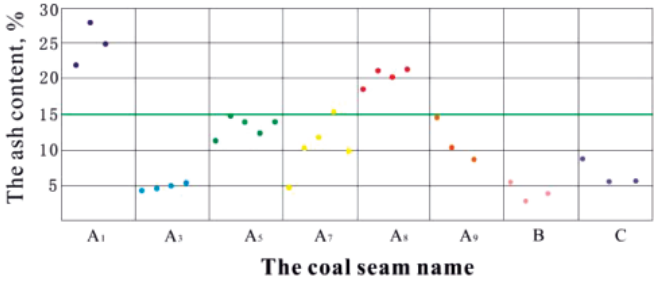

Fig.3 Scatter plot of the coal seam ash content

4.2. Pore structure characteristics of the coal seam

The low-temperature N_2 isotherm adsorption/desorption method is very effective in differentiating the transition pores and the micropores (Gurdal, G et al., 2001). The test result showed that the BET special surface area (S_{BET}) of the coal reservoir in the Kuba coalfield ranged from 0.0129 to 0.5329 m^2/g, with an average value of 0.3113 m^2/g; the BJH total pore volume (V_{BJH}) ranged from 0.000442 to 0.009755 mL/g, with an average value of 0.002462 mL/g; and the average pore diameter (D_{PORE}) was approximately 74.36 nm (Table 2). Compared to the Qinshui basin and the Lianghuai coalfield, the low-temperature nitrogen porosity characteristics in the coal reservoir of the Kuba coalfield are similar to those in these two blocks, and a large number of micropores had developed. However, the specific surface area and the total pore volume are slightly higher than those in the two former blocks; therefore, the coal reservoir in the Kuba coalfield has better gas storage capacity.

A change in the adsorption and desorption curve of the low-temperature nitrogen isotherm adsorption test can reflect the pore characteristics (Karl-Heinz et al., 2008). The curve of the sample in the study area is divided into two pore types; type A: the slope of the adsorption curve increased steadily and the pressure approached Po over time with varying

Table 2 Low-temperature N_2 isotherm adsorption/desorption test results

Target coal seams	Sample no.	S_{BET} m^2/g	D_{PORE} nm	V_{BJH} mL/g	Pore proportions %		
					>100 nm	10-100 nm	<10 nm
A_1	YZ001	0.5268	7.8435	0.009755	19.12	56.35	24.53
A_3	SF007	0.0356	136.1232	0.000890	22.85	50.71	26.44
A_5	WZ010	0.0129	160.9569	0.000442	32.92	51.47	15.61
A_7	WZ016	0.4335	41.9422	0.001385	29.63	52.71	17.66
A_8	CT021	0.3263	50.5281	0.001028	14.31	52.88	32.81
A_9	DWQ022	0.5329	48.7803	0.001272	21.79	57.20	21.01

S_{BET}: the BET special surface area; V_{BJH}: the BJH total pore volume; D_{PORE}: average pore diameter; mesopores (pore diameter•>100 nm); pores (pore diameter 10-100 nm); micropores (pore diameter•<10 nm).

steepness. The results show that this is a continuous pore system, and the desorption curve has an inflection point at a relative pressure of 0.5. The curve is divided into two sections, and the adsorption curve basically coincides with the desorption curve at a relative pressure of 0.5. According to the adsorption loop theory, the corresponding pores in this pressure section are mainly closed at one end, and at a relative pressure of 0.5.1.0. Obviously, the hysteresis ring of the adsorption loop shows that the corresponding pores in this pressure section are "ink bottle" type pores and partially open connected pores. The A_1, A_5, A_7 and A_8 coal seams belong to this type. In type B, the adsorption curve rises slowly, which indicates that the connectivity between pores is poor. The inflection point of the desorption curve is not obvious, the hysteresis loop is small, the pore types are mainly small pores and micropores, and the pore type increases sharply when the pressure is closed to Po. The pore type reflected is a plate hole, which is not open, and poor connectivity is observed, such as in the A3 and A9 coal seams (Fig.4).

The mercury intrusion method can quantitatively obtain the parameters when the pore diameter exceeds 7 nm, so this method has certain advantages in testing the pore structures of seepage pores. The characteristic parameters include the expulsion pressure, mercury intrusion saturation and extrusion efficiency. Generally, the lower is the expulsion pressure and the higher is the mercury intrusion saturation and extrusion efficiency, the better is the coal reservoir. The mercury intrusion saturation of coal reservoirs in the Kuba coalfield is generally low, which also shows that pore structures are mainly composed of micropores and pores, resulting in difficulties in the mercury vapour entering the seepage pores (Table 3). The mean range of the pore throat radius in the coal reservoir in the study area is 6.05–11.73 μm with an average of 8.93 μm, the average mercury saturation is approximately 79.81%, and the average mercury removal efficiency is approximately 52.56%. Experimental data on the mercury intrusion experiment of coal samples indicated that the porosity is relatively high, ranging from 5.01% to 10.03%. In the study area, the pores of coal reservoir are mainly adsorbed pores (micropores, pores). The pore structure is more disadvantageous from the point of view of coalbed methane development. In particular, the A_5 coal seam reservoir had a large amount of mercury and a high efficiency of mercury removal, which indicates that the pore development and connectivity are the best followed by those of the A_7 and A_9 coal seams.

4.3. Microfracture characteristics of the coal seam

The development of microfractures is restricted by the internal components of coal rocks, and development usually occurs in matrix vitrinite and homogenous vitrinite. When observed under a microscope, microfractures in the A1 coal sample are relatively undeveloped, and microfractures are mostly filled with inorganic minerals. The microfissures extended 1×10^4–1×10^7 nm, and the width is approximately 1×10^3–1×10^4 nm. The connectivity between the matrix pores and fissure system is not good, which is unfavourable for the development of coalbed gas migration. The A_3 coal

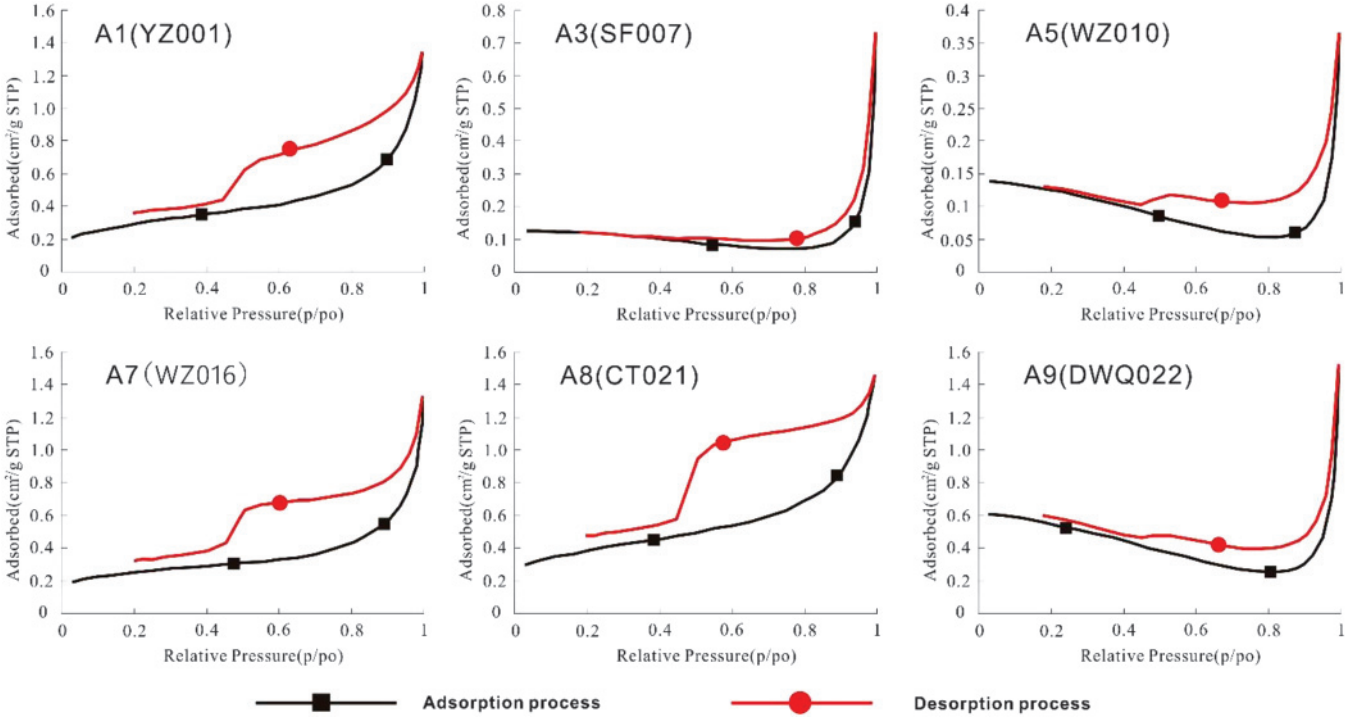

Fig.4 Isothermal adsorption line diagram of low-temperature nitrogen

TABLE 3 MERCURY INTRUSION RESULTS

Target coal seams	Sample no.	V_{in} %	V_{me} cm^3/g	E_{ex} %	P_{or} %	P_{ex} MPa	Content of pores%	
							P_{or} + P_{micro}	P_{meso}+ P_{macro}
A_1	YZ001	77.49	0.0113	61.08	5.01	0.01	73.06	26.94
A_3	SF007	82.84	0.0431	59.48	8.77	0.01	67.05	32.95
A_5	WZ010	90.45	0.0537	67.89	8.15	0.01	47.68	52.32
A_7	WZ016	88.11	0.0335	53.17	8.12	0.01	49.24	50.76
A_8	CT021	68.38	0.0737	51.95	9.61	0.01	59.89	40.11
A_9	DWQ022	91.71	0.0739	56.56	10.03	0.01	56.50	43.50
B	YZ025	70.62	0.2680	32.53	7.40	0.01	67.57	32.43
C	SF028	68.90	0.6860	37.82	11.64	0.02	63.32	36.68

V_{in}: maximum intrusion saturation; V_{me}: mercury intake; E_{ex}: extrusion efficiency; P_{ex}: expulsion pressure; P_{or}: porosity; P_{macro}: macropores; P_{meso}: mesopores; P_{or}: pores; P_{micro}: micropores.

microfractures had good connectivity between the matrix pores and fissure system. Powder is readily produced where microfractures develop, especially in the intersections of microfractures in different directions, and the coalbed gas migration pathway is easily blocked by the coal powder. Additionally, the cutting phenomenon of microcracks could be seen. The microfractures of A_5 coal are not developed, the connectivity between the matrix pores and fissure system is good, the powder production is lower in the microfissures, and the pyrite filled occasionally. The A_7 coal microfractures are less developed, and the connectivity is not good; the microfractures are mostly filled with calcite. The A_8 and A_9 coal microfractures are less developed, and the matrix pores and fissure system are well connected, which is favourable for the migration of coalbed gas. The microfracture has the phenomena of cutting and dislocating, and some microfractures are filled with quartz vein (Fig.5).

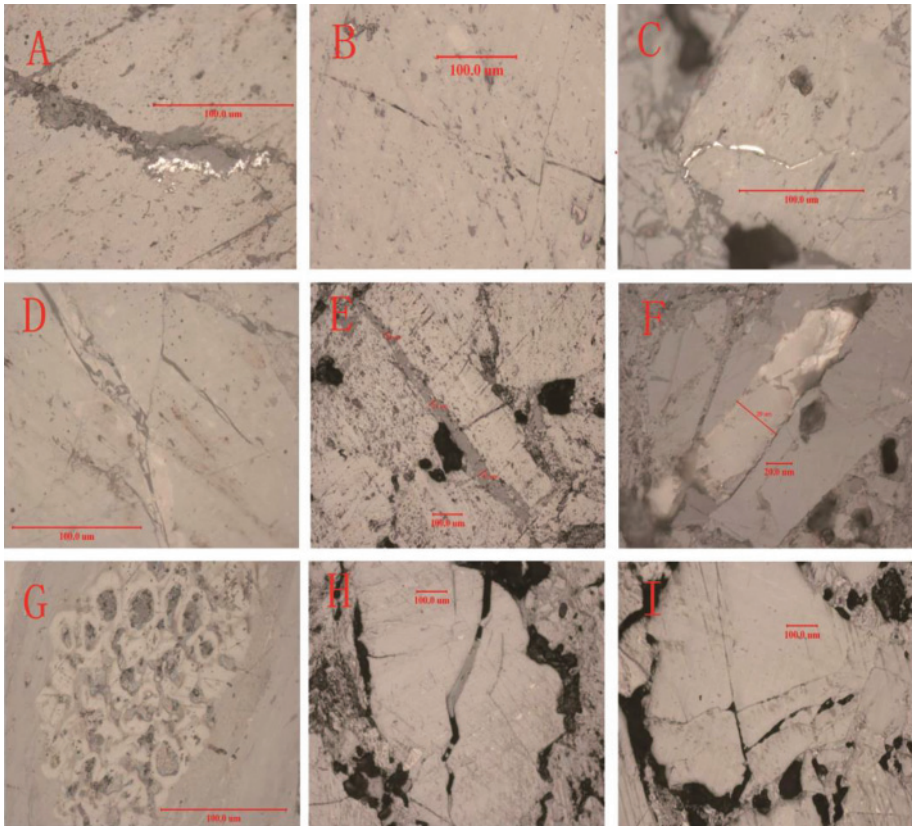

Fig.5 Microfractures in Kuba coalfield

Fractures have a fundamental influence on the permeability of the coal reservoir. The fractures in the study areas are divided into four types, A, B, C and D (Su et al., 2001; Yao et al., 2006; Solano Acosta et al., 2007; Li et al., 2012a): Type A with width (W) > 5 um and length (L) > 10 mm comprises fractures that can be distinguished clearly in macroscopic view. Type B with W > 5 um and 10 mm > L > 1 mm comprises continuous and long fractures. Type C with W < 5 um and 1 mm > L > 300 um comprises intermittent fractures, and type D with W < 5 um and L < 300 um comprises short fractures. The fracture frequency of the coal reservoir in the Kuba coalfield ranges from 91 to 485 per 9 cm^2 with an average value of 376 (Table 4). Types C and D are the leading fracture type, followed by type B, whereas type A is the least developed in the Kuba coalfield. The ratio of type D and C is approximately 90%, while that of type A and B is less than 10%. The proportion of microscopic fractures filled with minerals is between 5–42%, with an average of 26%. According to the degree of development of microfractures, the connectivity and filling ratio of the A_5 and A_7 coal seams

Table 4 Results of the fracture analyses of samples from the Kuba coalfield

Target coal seams	Sample no.	Fracture number per 9 cm^2					Fracture proportions %				Mineral filling microfractures	
		A	B	C	D	Sum	A	B	C	D	Filling umber per 9 cm^2	Proportions %
A_1	YZ001	4	29	172	154	358	1	8	48	43	136	38
A_3	SF007	6	79	217	277	579	1	14	37	48	245	42
A_5	WZ010	1	14	40	36	91	1	15	44	40	5	5
A_7	WZ016	2	54	93	108	257	1	21	36	42	20	8
A_8	CT021	0	51	162	213	426	0	12	38	50	102	24
A_9	DWQ022	0	44	238	204	485	0	9	49	42	150	31
B	YZ025	0	8	124	255	387	0	2	32	66	108	28
C	SF028	0	4	112	313	429	0	1	26	73	150	35

Table 5 Statistics of the macroscopic coal seam type

Target coal seams	Sample no.	Coal rock type ratio %				Evaluation type
		Bright coal	Semi-bright coal	Semi-dark coal	Dim coal	
A_1	YZ001	-	-	36	64	C
A_3	SF007	-	-	40	60	C
A_5	WZ010	-	57	29	14	A
A_7	WZ016	-	-	29	71	C
A_8	CT021	-	-	-	100	C
A_9	DWQ022	-	49	-	51	B
B	YZ025	-	-	70	30	C
C	SF028	-	40	-	60	B

are the most favourable followed by the A_3, A_8, A_9 and B coal seam. The A_1 and C coal seams are the most unfavourable for coalbed methane development.

4.4 Cleat characteristics of the coal seam

The inner fissure in coal is also called the cleat, and its development is mainly restricted by the composition of coal rock. Endogenous fissures are often found in bright coal rock composition-mirror coal and bright coal, often perpendicular to the stratigraphic surface, and the fissure surface is flat and is sometimes filled with mineral film. The brighter is the coal rock, the greater is the proportion of mirror coal and bright coal in the coal composition; on the contrary, the darker is the coal rock, the lower is the amount of mirror coal and bright coal. Measurements and statistics (Table 5) indicated that the density of endophytic fractures in the mirror coal bands of bright coal is 160–200 per m; in semi-bright coal bands, 120–150 per m; and in semi-dark coal, approximately 50–80 per m. The degree of development of endogenous fractures can be estimated and divided into three categories: class A: the proportion of bright and semi-bright coal in coal seams is high, generally higher than 50%, the proportion of dim coal is low, and the endogenous fractures are the most developed, for example, the A_5 coal seam. In class B, the proportion of bright and semi-bright coal in coal seams is generally less than 50%, the proportion of dim coal is higher than 50%, and the endogenous fissure is well developed, for example, the A_9 and C coal seams. In class C, the bright coal is not developed, i.e., there is mainly semi-dark coal and dim coal; the proportion of dim coal is generally higher than 60%; and the endogenous fissures are not developed, such as in the A_1, A_3, A_7, A_8 and B coal seams. Therefore, from the perspective of the development of endogenous fractures, coal seam A_5 is favourable for the development of coalbed methane.

4.5 Exogenetic fracture characteristics

Based on the mapping of outcrop structural fractures in the field and the fine contrast technique of coal reservoirs under coal mines, a total of 4405 joints are measured in the study area. The exogenetic fracture produced by tectonic stress is not only found in coal rock but also in surrounding rock. It is the main channel of coalbed methane migration and seepage flow, which is the dominant direction of permeability. The outcrops of coal reservoirs are observed on the surface of the study area. It was found that all directions of exogenetic fractures were developed, but three dominant directions are mainly developed, that is, the dominant strike is in the direction of NNW, NNE and SN. Generally speaking, A_5 and A_7 coal seams have better development of exogenous fractures than A_2 and A_3 coal seams, and A_1 coal seams have the worst development. Therefore, A_5 and A_7 coal seams are more favourable for CBM development.

5. Conclusions

This work aimed at studying pores and microcracks in the coal reservoir of the Kuba coalfield. Moreover, the internal and external fractures are studied by using structural fissure mapping and comparative anatomy of the underground coal reservoir in order to examine the pores in the coal reservoir. The fractures are studied as an organic whole from micro to macro fractures. Through comprehensive research, the coal reservoir is selected from the perspective of pores and fissures. Details of the results obtained in this study are summarized as follows:

1. The results indicate that the A_1 and A_8 coal reservoirs are not favourable for coalbed methane development. Specifically, the ash content of the other coal seams studied is less than 15%, which is more appropriate for the development of coalbed methane. This study concluded that the coal reservoirs of A_5 and A_7 in the Kuba coalfield are the most appropriate for the development of coalbed methane.
2. Experimental data on the mercury intrusion experiment of coal samples indicated that the pores of coal reservoir are mainly adsorbed pores (micropores, pores). The pore structure is more disadvantageous from the point of view of coalbed methane development.
3. According to the degree of development of microfractures, the connectivity and filling ratio of the A_5 and A_7 coal seams are the most favourable followed by the A_3, A_8, A_9 and B coal seams. Additionally, it is shown that the A1 and C coal seams are the most unfavourable for coalbed methane development.
4. From the perspective of the development of endogenous fractures, the coal seam A_5 is more favourable for the development of coalbed methane.
5. A total of 4405 flat, extended, and mainly flat joints are measured in the study area. A_5 and A_7 coal seams have better development of exogenous fractures than A_2 and A_3 coal seams, A_1 coal seams have the worst development.

References

[1] Gamson, P.D., Beamish, B.B., Johnson, D.P., 1998. Effect of coal micro-structure and secondary mineralization on methane recovery. Geological Special Publication 199 (1), 165-179.

[2] Shi, J.Q., Durucan, S., 2005. Gas storage and flowin coalbed reservoirs: implementation of a bidisperse pore model for gas diffusion in a coal matrix. SPE (Society of Petroleum Engineers) *Reservoir Evaluation & Engineering* 8 (2), 169-175.

[3] Xu, H., Zhang, S.H., Leng, X., Tang, D.Z.,Wang, M.S., 2005. Analysis of pore system model and physical property of coal reservoir in the QinshuiBasin. *Chinese Science Bulletin* 50, 45-50.

[4] Yao, Y.B., Liu, D.M., Tang, D.Z., Tang, S.H., Huang, W.H., Liu, Z.H., Che, Y., 2009. Fractal characterization of seepage-pores of coals from China: an investigation on permeability of coals. *Computer and Geo-sciences* 35 (6), 1159-1166.

[5] Ayers Jr., W.B., (2002): Coalbed gas systems, resources, and production and a review of contrasting cases from the San Juan and Powder River basins. *AAPG Bull*. 86(11), 1853-1890.

[6] Sang, S., Zhu, Y., Zhang, J., Zhang, X., Tang, J., (2005): Solide gas interaction mechanism of coal-absorbed gas (I)-coal pore structure and solid-gas interaction. *Nat. Gas. Ind.* 1, 004.

[7] Li, S., Tang, D., Pan, Z., Xu, H., Huang, W., (2013): Characterization of the stress sensitivity of pores for different rank coals by nuclear magnetic resonance. *Fuel* 111, 746-754.

[8] Li, S., Tang, D., Pan, Z., Xu, H., (2014a): Influence and control of coal facies on physical properties of the coal reservoirs in western Guizhou and eastern Yunnan, China. *Int. J. Oil Gas Coal Technol*. 8, 221-234.

[9] Moore, T.A., (2012): Coalbed methane: a review. *Int. J. Coal Geol.* 101, 36e81.

[10] Law, B.E., (1993): The relation between coal rank and cleat spacing: implications for the prediction of permeability in coal. Proc. Int. Coalbed Methane Symp. II, 435-442.

[11] Xue, G., Liu, H., Li, W., (2012): Deformed coal types and pore characteristics in Han-cheng coalmines in Eastern Weibei coalfields. *Int. J. Min. Sci. Technol*. 22, 681-686.

[12] Zhang, Z., Wang, S., Wang, X., (2016): Physical Characteristics of Coal Reservoir and Prospects in Exploration and Development of Kuqa-Bay Coalfield, Xinjiang. *J. Coal Technology.* 35, 117-119.

[13] Tang, S., Sun, S., Hao, D., Tang, D., (2004). Coalbed methane-bearing characteristics and reservoir physical properties of principal target areas in North China. *Acta Geol. Sin*. 78, 724-728.

[14] Li, G., Zhang, H., (2013): The origin mechanism of coalbed methane in the eastern edge of Ordos Basin. *Sci. China Earth Sci.* 8, 1359-1364.

[15] Meng, Y., Tang, D., Xu, H., Li, C., Li, L., Meng, S., (2014): Geological controls and coalbed methane production potential evaluation: a case study in Liulin area, eastern Ordos Basin, China. *J. Nat. Gas Sci. Eng.* 21, 95-111.

[16] Cai, Y., Liu, D., Yao, Y., Li, J., Qiu, Y., (2011): Geological controls on prediction of coalbed methane of No. 3 coal seam in Southern Qinshui Basin, North China. *Int. J. Coal Geol*. 88, 101-112.

[17] Tao, S.,Wang, Y., Tang, D., Xu, H., Lv, Y., He,W., Li, Y., (2012): Dynamic variation effects of coal permeability during the coalbed methane development process in the Qinshui Basin, China. *Int. J. Coal Geol*. 93, 16-22.

[18] LV, Y., Tang, D., Xu, H., Luo,H., (2012): Production characteristics and the key factors in high-rank coalbed methane fields: a case study on the Fanzhuang Block Southern Qinshui Basin, China. *Int. J. Coal Geol.* 96, 93-108.

(Continued on page 191)